Al-fumarate, a Metal-Organic Framework encapsulating antigen as a potent, versatile and resorbable vaccine adjuvant

Ioanna Christodoulou,[1,±] Effrosyni Gkaniatsou,[1,±] Flavien Bourdreux,[1] Mohamed Haouas,[1] Nathalie Steunou,[1] Gilles Patriarche,[2] Chakib Djediat,[3] Aurélie Pagnon-Minot,[4] Charlotte Lecerf,[5] Marion Lopez,[5] Emmanuel Chereul,[5] Brigitte Reveil,[6] Sandra Audonnet,[7] Aymric Kisserli,[6,8] Thierry Tabary,[6] Jacques H.M. Cohen,[6,*] and Clémence Sicard[1,9*]

[±] *contributed equally*

[1] *Institut Lavoisier de Versailles, UMR CNRS 8180, UVSQ, Université Paris-Saclay, 78035 Versailles, France*

[2] *Centre de Nanosciences et de Nanotechnologies (C2N), Université Paris-Saclay - CNRS, 91120 Palaiseau*

[3] *Muséum National d'Histoire Naturelle, UMR CNRS 7245, Bâtiment 39, CP 39, 57 rue Cuvier, 75231, Paris, France.*

[4] *Novotec, ZAV du Chêne, Europarc, 11 rue Edison, Bron 69500, France*

[5] *Voxcan, 1305 Route de Lozanne, 69380 Dommartin, France*

[6] *Nanosciences Research Laboratory LRN EA 4682, University of Rheims Champagne-Ardenne, Rheims, France*

[7] *URCACyt, Flow Cytometry Technical Platform, University of Rheims Champagne-Ardenne, Rheims, France*

[8] *Oncogeriatric Coordination Unit, Rheims University Hospital, Rheims, France*

[9] *Institut Universitaire de France*

For correspondence: jhmcohen@gmail.com and clemence.sicard@uvsq.fr

Abstract

Although used for one century in billions of people as the vaccine adjuvant with the best benefit/side-effect balance, aluminium salts/gels have drawbacks of rapid leakage of antigens from the injection site and indefinite persistence. Herein, we propose an alternative to canonical Al-adjuvant. Proteins, nucleic acids, and bacteria were successfully encapsulated within an Al-based Metal-Organic Framework (MOF), namely Al-fumarate, using a synthesis process in water and room temperature, compatible with bio-entities preservation. Mice immunizations demonstrated antigenicity preservation of tetanus toxoid and inactivated *E. coli*, and a stronger adjuvant effect of Al-fumarate than benchmark Al-adjuvant (Alhydrogel) with an initial slow antigen release and a protective effect. The Al-fumarate vaccine formulation was fully resorbable *in vivo*, disappearing from the injection site, was not exhibiting any toxicity, and was stable for two years. The limitation of Al adjuvants as eliciting only antibody responses was also overcome by co-immobilisation of CpG 1018 with tetanus toxoid.

Keywords: Metal-Organic Framework, Encapsulation, Antigen, Adjuvant, Vaccine

Introduction

Vaccines are powerful means for managing and preventing the spread of pathogens and infectious diseases worldwide and the best-cost effective tool for public health, particularly in avoiding numerous deaths among children.[1] Prophylactic vaccines categorized into living, non-living, and nucleic acid ones are administrated to healthy populations and should be extremely safe with minimal side-effects.[2] Non-living vaccines, made from non-infectious or inactivated forms of antigens, require the use of an adjuvant to obtain long-lasting efficient immune coverage against targeted pathogens or diseases.[3,4] Al-based salts or gels (mainly aluminium (oxo)hydroxide or phosphate) remain the leading adjuvants in humans vaccination. They have been administrated to billions of individuals for a century,[5] due to their unique ability of inducing sustainable and neutralizing antibodies for many inactivated antigens such as toxoids.[6,7] Even if their clinical efficiency to side effect ratio is undoubtedly proven excellent, these adjuvants still have some limitations: *(i)* They, in part, can remain indefinitely at the injection site.[8–10] This situation has led to vaccine reluctance on a part of the general public due to a fear of Al vaccines owing to the inaccurate correlation between the low Al amounts in vaccines (typically 0.5 mg per injection)[11] with the Al induced encephalopathy cases;[12,13] *(ii)* They only induce humoral immune responses that can be ineffective against some infectious agents and irrelevant for most cancer immunotherapy;[14] *(iii)* They can exhibit an initial rapid leakage of soluble antigens, reducing the overall immune potency;[15] *(iv)* They are incompatible with some fragile antigens that can be denatured.[16] *(v)* Mixture adjustments in multi-valent vaccines may be challenging, owing to the specific nature of adjuvant-antigen correlation.[17] The first two drawbacks are mostly related to the chemical composition of the adjuvant, while the others result mainly from the antigens immobilization process based on surface electrostatic adsorption or ligand exchange. A myriad of alternative adjuvants has been developed either with different chemical compositions (e.g. Freund's adjuvant, squalene, liposomes, MF59, lipids, cell exosomes or bacteria wall, etc),[18–27] or structurally different Al-based adjuvants,[15,28] but only a few have reached approval for human use as many exhibit either unacceptable side effects, insufficient immune responses, stability issues or difficulties in scaling-up.[29–32] Alternatively, the lack of cellular response in traditional Al-adjuvants can be compensated by the addition of immune orienteers (oligonucleotides,[33] imidazoquinoline,[34] TLR7 agonists[35]). Due to the inefficient retention of such orienteers by Al salts and their rapid leakage from the injection site, this approach can however demand high dosages that in some cases can lead to

significant toxicities which may be acceptable for cancer immunotherapy but not for prophylactic vaccination.[35]

To overcome some limitations of canonical Al-adjuvants while preserving their strength and effectiveness, we propose a different approach that consists of entrapping antigens (together with if necessary immune orienteers) within a resorbable Al-based Metal-Organic Framework (MOF). MOFs are built-up from inorganic and organic building units forming three-dimensional crystal structures of high surface area and porosity.[36,37] For biomedical applications, such as drugs,[46] gases,[47] proteins[38] or nucleic acid[39] delivery, MOFs exhibited appealing properties, including controlled release, *in vivo* degradation, and low toxicity.[40] For such applications MOFs with non-immunostimulant properties were preferentially considered (*i.e.* Fe-, Zr- or Zn-based). Only recently, their potential inherent immunogenicity was investigated.[41] They revealed of interest for immunotherapy,[42,43] mainly as cargo for oligonucleotides.[44–47] For vaccination, similarly, the role of MOFs has been mostly restricted to an antigens and adjuvants carrier rather than actively participating in an immunostimulant action.[48–57] Very few works have used Al-based MOFs both as the antigen cargo and adjuvant by itself.[58,59] But the antigens' immobilization was performed similarly to canonical Al-adjuvants by surface electrostatic adsorption onto preformed particles. Interestingly, encapsulation of antigens in Zn-based MOFs[60] provided a protective armour that favours the immune response by limiting antigen leakage or degradation and by depot effect even in the absence of a direct adjuvant effect of the metal used.[61–63]

Herein, we report the entrapment of antigens within Al-fumarate,[64] an Al-MOF (Fig. 1a), the MOF assembly being performed in presence of antigens using non-denaturing conditions for biological entities (water, room temperature). Fumarate was selected as the MOF's organic ligand as it is an endogenous molecule involved in the Krebs cycle and thus atoxic.[65] The relevance of the process was evidenced in terms of *in vivo* adjuvant potency, resorption, tolerance, long-term stability, and slow antigen initial release. We demonstrate the suitability and universality of this approach for various antigens ranging from soluble proteins (tetanus toxoid) to bacteria (*Escherichia coli*), as well as the possibility to co-immobilise antigens with an oligonucleotide immune orienteer (CpG 1018).

Results and discussion

Vaccine formulations

The synthesis of the aluminium polycarboxylate MOF, Al-fumarate, $Al(OH)(C_4H_2O_4)$ (Fig. 1a),[64] was optimized to be performed in conditions non-denaturing for antigens, *i.e.* aqueous media, room temperature (SI section 2A). An 8-hour reaction protocol enabled to reach equilibrium and recover Al-fumarate (Fig. S1-S3). The characteristic Bragg peaks of the PXRD pattern were relatively broad, this being attributed to small particle size and low crystallinity as Al-fumarate is well-known to give poorly crystallized particles (Fig. 1c-d).[64,66] The stability of Al-fumarate in common vaccine injection media was assessed and HEPES buffer (20 mM, pH 7.4) was selected to formulate Al-fumarate vaccines (SI section 2B, Fig. S4-S8).

Tetanus Toxoid (TT) was first selected as a well-known antigen model, extensively studied, and used in commercial vaccines.[67] Vaccines were formulated at two TT concentrations based on the human tetanus vaccine model: C0 (3.2 IU, 78.4 µg/ml TT) and C1 (1.6 IU, 39.2 mg/ml TT) with the same TT/Al ratio (0.08 IU/µg Al) (Fig. 1b).[68] TT was immobilized within Al-fumarate by introducing the antigens during the MOF synthesis (see experimental section). The presence of TT did not affect the MOF crystallinity, nor the particles' morphology (individual rod-shaped nanoparticles of around 13 ± 5 nm by 40 ± 10 nm, forming aggregates of 100 nm to few µm) (Fig. 1c-d, SI section 3A, Fig. S9-S12). No residual TT was detected in the synthesis supernatants, confirming the total immobilization of the antigen (Fig. S13). Confocal laser microscopy imaging using fluorescence-labelled TT confirmed its homogenous distribution throughout the particles (Fig. S14). The stability of the vaccine formulation over one week was confirmed based on the absence of TT leaching (Fig. S15), in agreement with the stability of Al-fumarate in HEPES buffer.

For comparison sake, vaccine formulations using Alhydrogel ($Al(OH)_3$), the commercial benchmark aluminium adjuvant, were also prepared at C0 and C1 concentrations with identical TT/Al ratio (see experimental section). The amount of aluminium was similar for TT@Al-fumarate and TT-Alhydrogel (Table S3-S5).

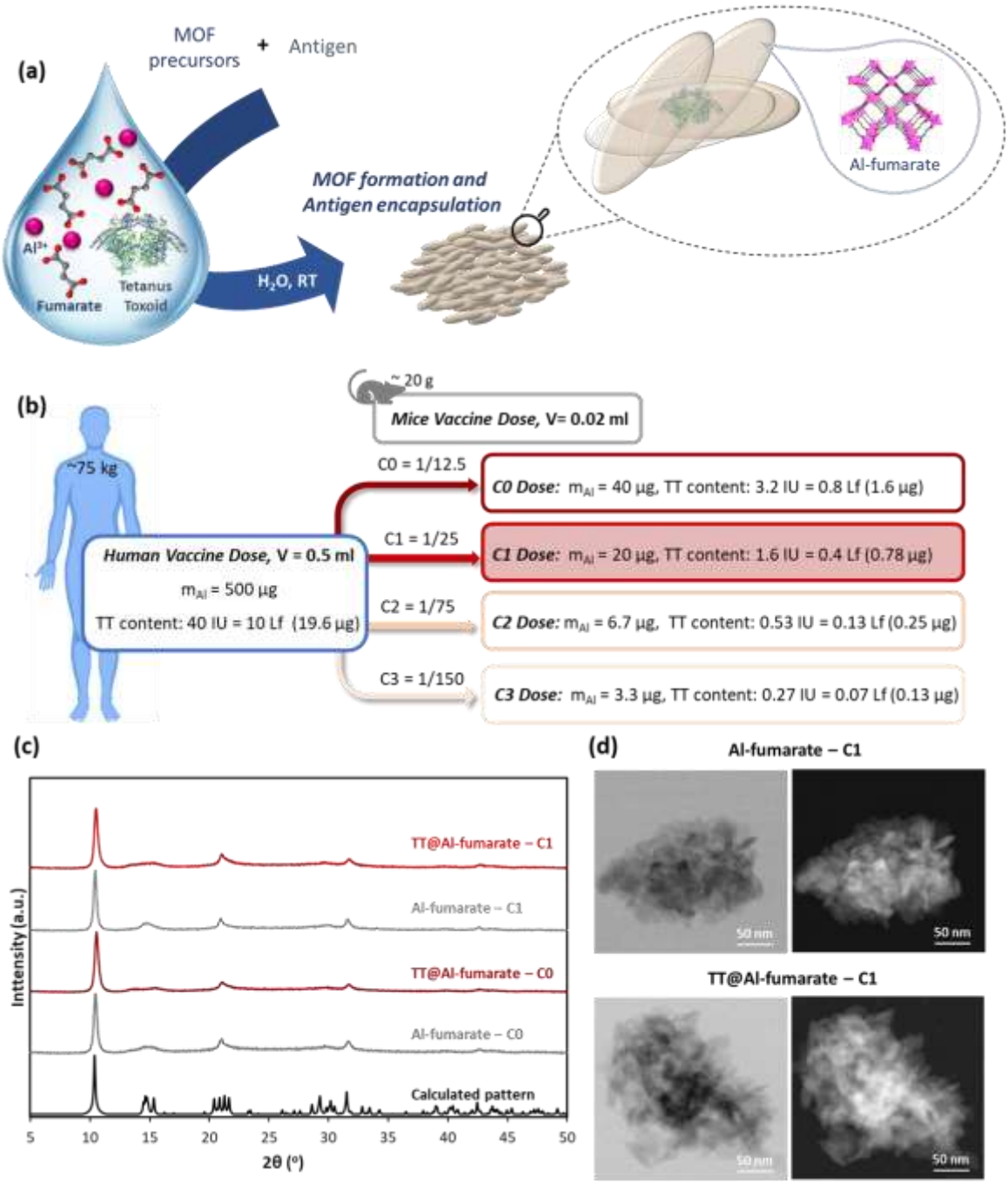

Figure 1. ***(a)*** *Schematic representation of the antigen entrapment process. Al-fumarate is built up from chains of corner sharing AlO_6 octahedra connected through fumarate ligands and μ_2-OH bridges to define diamond shaped channels of ~6 Å free diameter.* ***(b)*** *Mice vaccine doses based on tetanus toxoid monovalent human vaccine dose.*[68] *All vaccines were formulated with the same TT/Al ratio of 0.08 IU/µg Al. IU represents international unit of antigen activity, also expressed in Lf (Limit of Flocculation). The TT solution used for the synthesis was at 2.8 mg/ml and 1428 Lf/ml.* ***(c)*** *Powder X-Ray Diffraction patterns of Al-fumarate calculated (obtained from CCDC, deposition number: 1051975, database identifier: DOYBEA) and experimental Al-fumarate and TT@Al-fumarate (C1 and C0 concentrations). λ = 1.5406 Å* ***(d)*** *Bright Field STEM (left column) and STEM-HAADF (right column) images of Al-fumarate (top row) and TT@Al-fumarate (bottom row) (C1 concentration).*

Immunizations and Antibody responses

In order to quantitatively assess the effect of the two adjuvants, a sub-optimal single injection protocol in mice, an immunocompetent species poorly responding to TT, was chosen. Balb/c mice were immunized by 20 µl intramuscular (IM) injections in the right hind-limb. Initially, the immune response against formulations at four concentrations (C0 to C3, Fig. 1b) was evaluated quantitatively by the anti-TT IgG antibody titers in mice sera one month after immunization (SI section 1C). TT@Al-fumarate formulations resulted in greater antibody titers than those obtained with TT-Alhydrogel formulations for all four concentrations (Fig. S16). The C1 concentration was subsequently selected for a longitudinal study with antibody titration at 14 and 32 days. At both time-point, TT@Al-fumarate induced a significant higher anti-TT IgG antibody level than TT-Alhydrogel (Fig. 2a). Comparison of anti-TT whole Ig dilution curves showed, at each tested dilution, a clear stronger Ig response induced by TT@Al-fumarate over TT-Alhydrogel (Fig. 2b). Under all the tested conditions, TT@Al-fumarate exhibited a more potent immune response, indicating a higher adjuvant effect of the Al-fumarate MOF than the reference Al-adjuvant.

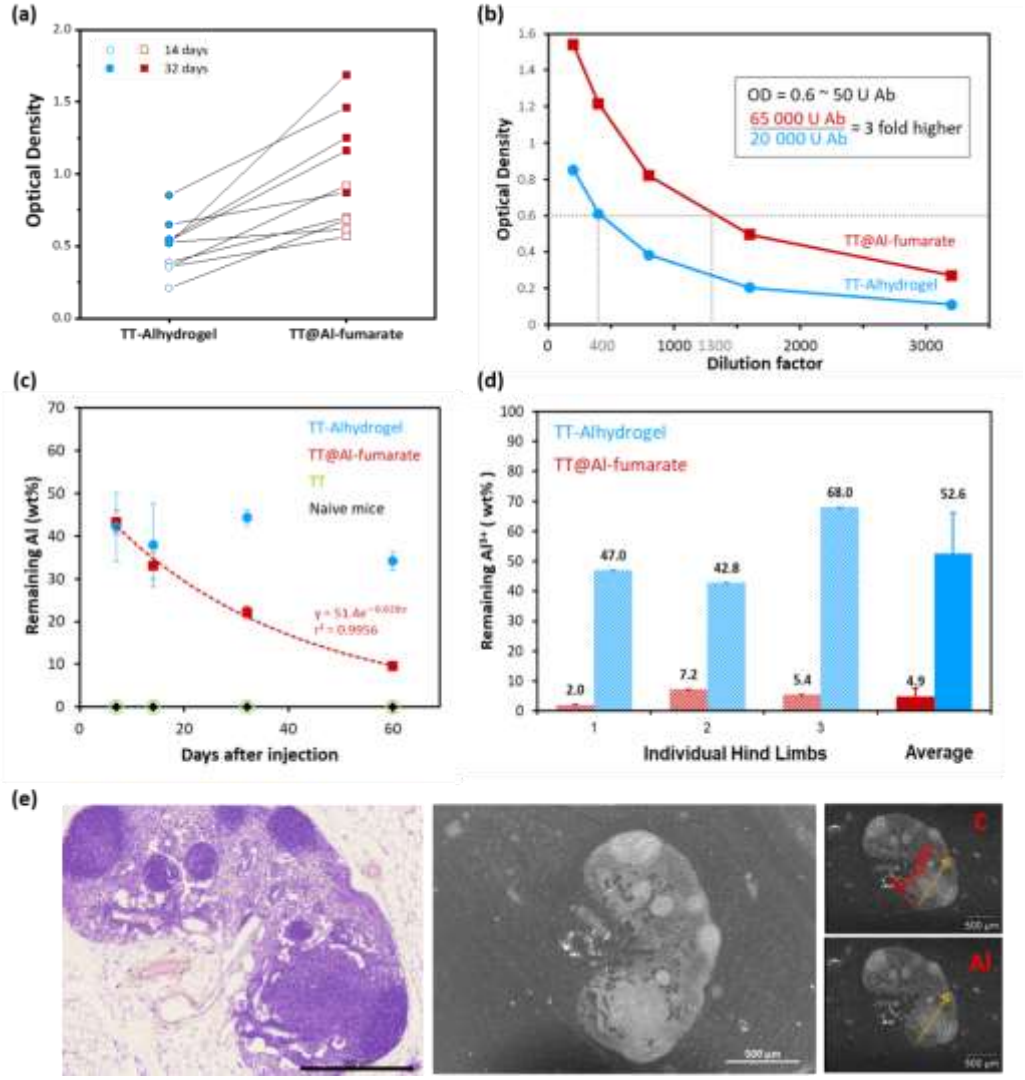

Figure 2. (a) *Comparison of 10 paired anti-TT IgG immune responses induced in Balb/c mice by TT-Alhydrogel (blue circle) and TT@Al-fumarate (red square) at D14 (open symbols) or D32 (full symbols) after injections with C1 concentration (20 µl C1 concentration, IM, right hind-limb,). Optical density (OD) was observed on the same ELISA plates for paired sera diluted to 1:1000. **p < 0.01 as determined by Wilcoxon Signed Ranks Test.* ***(b)*** *Ig anti-TT ELISA OD comparison of representative dilution curves of mice sera (pooled sera from 2 mice ranking 3 and 4 in each mice group) obtained at D32 either following immunization by TT-Alhydrogel (blue circle) or TT@Al-fumarate (red square). Insert: comparison of values at OD = 0.6 expressed in kU from the reference curve of the ELISA kit (reference curve is depicted in Fig. S17).* ***(c)*** *Remaining aluminium at the injection site measured at 7, 14, 32 and 60 days after injection of TT, TT-Alhydrogel or TT@Al-fumarate (20 µl C1 concentration, IM, right hind-limb, N=5). Error bars represent the standard error of the mean.* ***(d)*** *Aluminium remaining at the injection site 90 days after injection (50 µl C1 concentration, IM, hind-limb). Three individual paired values (left) and mean value (right).* ***(e)*** *Tissue section stained in HES of a representative inguinal lymph node draining the IM injection site of TT@Al-fumarate at D32. From left to right: HES staining, SEM and EDS analysis of C and Al elements. Scale bars represent 500 µm.*

Resorbable character

To assess the resorbable character of the adjuvants, the amounts of Al^{3+} deriving from the digested right limbs of mice injected with 20 µl C1 concentration (20 µg Al) either as TT@Al-fumarate or TT-Alhydrogel were quantified by ICP-OES (Fig. S18). The deducted Al^{3+} wt% remaining at the injection site is presented in Fig. 2c. For both adjuvants at day 7, less than half of the injected aluminium remained at the injection site (~ 43 wt%). From day 14, a gradual decrease of the aluminium from TT@Al-fumarate could be observed, whereas the aluminium from TT-Alhydrogel remained at the injection site as shown by the constant amounts of detected Al^{3+}. At day 60, the mice injected with TT-Alhydrogel presented 3.6 times more aluminium than the mice injected with TT@Al-fumarate (~ 10 wt%). Half-life of aluminium from TT@Al-fumarate (determined starting from day 7) was of ca. 25 days whereas aluminium from the TT-Alhydrogel being almost constant displayed an apparent half-life of more than 220 days.

To confirm that the aluminium decay followed a 1st order kinetic law and was quantity-independent, a similar study was conducted with higher injected amount (50 µl C1 per hind-limb, 50 µg Al, Fig. 2d and S19). At day 60, 8 wt % of injected aluminium remained at the injection site for the mice injected with TT@Al-fumarate, in accordance with the value obtained with lower dose. At day 90, the mice injected with TT-Alhydrogel presented 10 times more aluminium at the injection site than the mice injected with TT@Al-fumarate for which only 5 wt% of the injected aluminium remained at the injection site.

These results confirmed the local persistence of a part of the reference Al-adjuvant as well as the disappearance within a few months of Al-fumarate MOF. Despite the recognized safety profile of the reference Al-adjuvant, as a result of its immunostimulant character and persistence, on rare occasions macrophage granulomas can developed within the muscle tissue at the injection site (Fig. S20).[8–10] The disappearance of the injected aluminium should avoid such phenomena and be a strong reassuring argument for the general public. It could be also advantageous from a pharmaceutical point-of-view since the totality of the injected adjuvant serves as a vehicle for antigen presentation to the antigen presenting cells (APC) in contrast to insoluble remaining aggregates of the reference Al-adjuvants.

Note that no excess of aluminium was detected in the blood circulation of any mice group (Table S6) or stored in storage organs such as liver and spleen, even when high aluminium amount (200 µl C1 concentration, 200 µg Al) was injected (Table S7), indicating the absence of Al^{3+} circulation or retention in the body and suggesting its fast excretion.

It should also be kept in mind that once initiated a large part of the immune response is no longer developing at the injection site but in the regional lymph node, as illustrated by the very

active inguinal lymph node draining the injection site where Al was not found using EDS analysis (Fig. 2e and S21). In a high dose study (100 µl C1 sub-cutaneous injection), a grade 1 transient macroscopic local reaction was observed at day 15 that quickly disappeared in less than a month. Taken together with the stronger antibody responses observed using the resorbable Al-fumarate MOF adjuvant, these data revealed, as already observed,[69,70] that specific immune response is not a long lasting focal phenomenon at the injection site, and that the long term persistence of $Al(OH)_3$ is not needed for a strong antibody production.

Safety of the TT@Al-fumarate vaccine formulation

Throughout the course of all mice studies, no behaviour or animal growth abnormality was observed (Fig. S22). When a high dose was injected (200 µl at C1 per mouse equivalent to 2/5th of a human dose in a 20 g mouse, SI section 1C), similar results were observed (Fig. S23). Local reactions were null or only reaching a grade 1 transient local swelling in the high dose study. Histological observations of spleen, liver and kidney did not reveal any abnormal cells nor any difference between tissues from TT@Al-fumarate injected mice and naïve mice (Fig. 3a). The Al-fumarate adjuvant did not induce any acute toxicity.

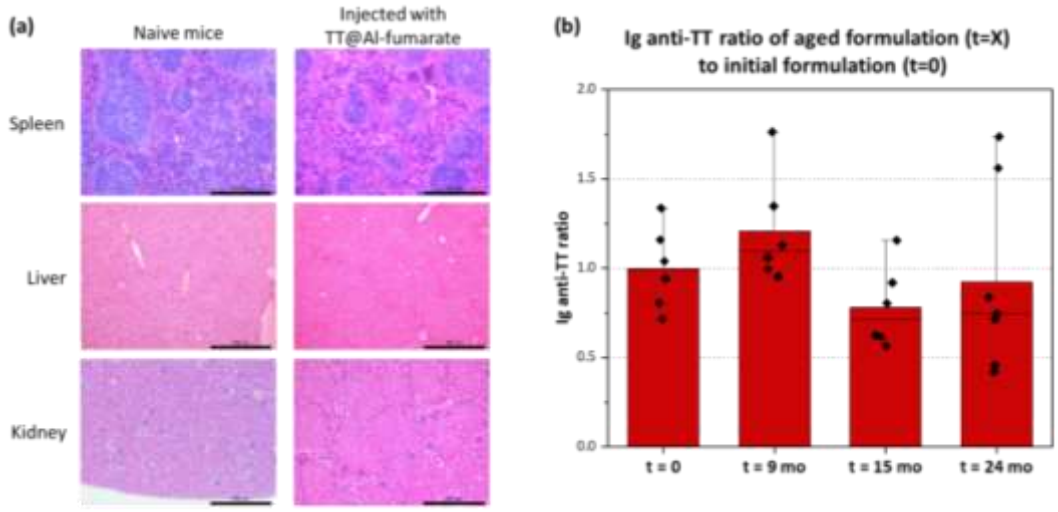

Figure 3. (a) *Spleen, liver, and kidney tissue section (HES staining) from naïve mice (left column) and mice immunized IM with TT@Al-fumarate (right column). Spleen and liver were harvested 7 days after injection of a total of 200 µl at C1 concentration. Kidneys were harvested 35 days after injection of 35 µl at C1 concentration. Scale bar represents 500 µm.* ***(b)*** *Stability of TT@Al-fumarate as immunogen. A single preparation of TT@Al-fumarate was tested at 9, 15, and 24 months by comparing anti-TT Ig antibody levels obtained from the initial preparation (t=0) to sample kept à 4 °C (t=X). Sera diluted 1:1000. Histograms represent the mean values, black solid lines represent the median values, and diamond shapes represent individual mice. Anti-TT Ig antibody levels between formulations were non-significantly different with p > 0.13 as determined via Tukey's correction as part of a one-way ANOVA.*

Long-term storage stability and repeatability of TT@Al-fumarate vaccine formulation

The repeatability of the formulation was assessed by comparing 4 different preparations of TT@Al-fumarate prepared by 2 different individuals (Table S8). Similar antibody responses were obtained (Fig. S24), indicating the robustness of the process.

The TT@Al-fumarate vaccine formulation was stored at 4 °C without any preservative and was injected 9, 15 and 24 months after preparation. The comparison of the Ig levels obtained with aged formulations versus the initial formulation prepared at t=0 did not show any decrease in the immunogenic properties (Fig. 3b), demonstrating the stability of the formulation over at least 24 months. This high stability reaches the regulatory requirements for the pharmaceutical industry. Noticeably, a decay of immunogenicity was observed with formulations prepared from non-encapsulated aged TT (Fig. S25), suggesting a protective and stabilizing effect of the encapsulation.

Factors contributing to the enhanced immune response of TT@Al-fumarate

To follow the antigen availability and kinetics, TT was labelled with a NIR fluorophore (InvivoTag 680, SI section 1A). Three formulations (fluo-TT@Al-fumarate, fluo-TT-Alhydrogel and fluo-TT) were prepared such as all mice were IM injected with 4 IU fluo-TT and comparable Al content for the adjuvanted formulations (SI section 1C, Fig. S26 and Table S9). Despite preliminary *in vitro* studies revealed a strong quenching of the fluorescent signal when fluo-TT was immobilized within the MOF (Fig S27), the radiance signal was more than one Log above the control background, allowing a longitudinal study for almost a month (Fig. 4a-b and Fig. S28). After 28 days, the remaining focal fluo-TT was almost negligible for fluo-TT without adjuvant (< 5 %), only 11 % for fluo-TT-Alhydrogel and 16 % for fluo-TT@Al-fumarate groups. Interestingly, when comparing with the 44 % and 22 % aluminium amount remaining after one month for TT-Alhydrogel and TT@Al-fumarate, respectively (Fig. 2c), it suggested that contrary to Alhydrogel adjuvant, a concurrent release of TT and Al is observed in the case of Al-fumarate, which may improve the immune response.

The fluorescence decay kinetics were evaluated (Fig. 4b-c). During the first 8 days, decay of fluo-TT without adjuvant followed a single exponential curve, with a half-life of 4.08 days, whereas decay of fluo-TT@Al-fumarate was the longest (6.86 days), fluo-TT-Alhydrogel displaying an intermediate half-life (5.37 days). Considering 16 days period, half-life of fluo-TT remained constant (4.10 days) while half-life of fluo-TT@Al-fumarate decreased to 5.29 days, suggesting a dual decay. This dual decay revealed a slower release of TT at the early time of the immune response, followed by a faster TT release.

Fluo-TT-Alhydrogel decay curve also exhibited a dual decay (half-life of 4.65 days on 16 days), but with a smaller initial slow release effect than fluo-TT@Al-fumarate. The persistence of antigens at the injection site in the first days following injection (also called depot effect), may be key to a strong immune response.[71–73] We can thus assume that the better adjuvant efficiency of TT@Al-fumarate might also be linked to more favourable antigen release kinetics, making it more available at the injection site during the first days of the immune response.

Remarkably, upon examination of the remaining aluminium amount 7 days after injection, the residual fluo-TT to aluminium ratio was about 0.8 and 1.2 for Alhydrogel and Al-fumarate adjuvants, respectively. In the first days, in the case of Al-fumarate, aluminium is thus released in slight excess to TT, supporting the hypothesis that aluminium is available simultaneously to the release of TT which probably is also contributing to the improved immune response observed using Al-fumarate.

The importance of the encapsulation process was also investigated and compared with a physical adsorption of TT on preformed MOF particles (TT-on-Al-fumarate, see experimental section, SI section 9, Fig. S29-31). TT, TT@Alhydrogel, TT@Al-fumarate and TT-on-Al-fumarate vaccines were formulated at the C1 concentration, and for the three adjuvants with identical Al content (Table S10). As expected, Ig levels obtained with TT@Al-fumarate were significantly higher than those obtained with TT@Alhydrogel, and those obtained with TT without adjuvant (Fig. 4d). Interestingly, Ig levels obtained with TT-on-Al-fumarate were lower than levels obtained with TT@Al-fumarate, and similar to levels obtained with the reference adjuvant TT-Alhydrogel (similar results were obtained with IgG levels). These results indicate that the encapsulation of TT during the MOF formation rather than its surface immobilization, improves the antigen immune efficiency.

All these data suggest that the enhanced immune response obtained with the MOF matrix resulted probably from the combination of a slow antigen release in the first days with a concurrent release of Al from Al-fumarate and an *in vivo* protection effect.

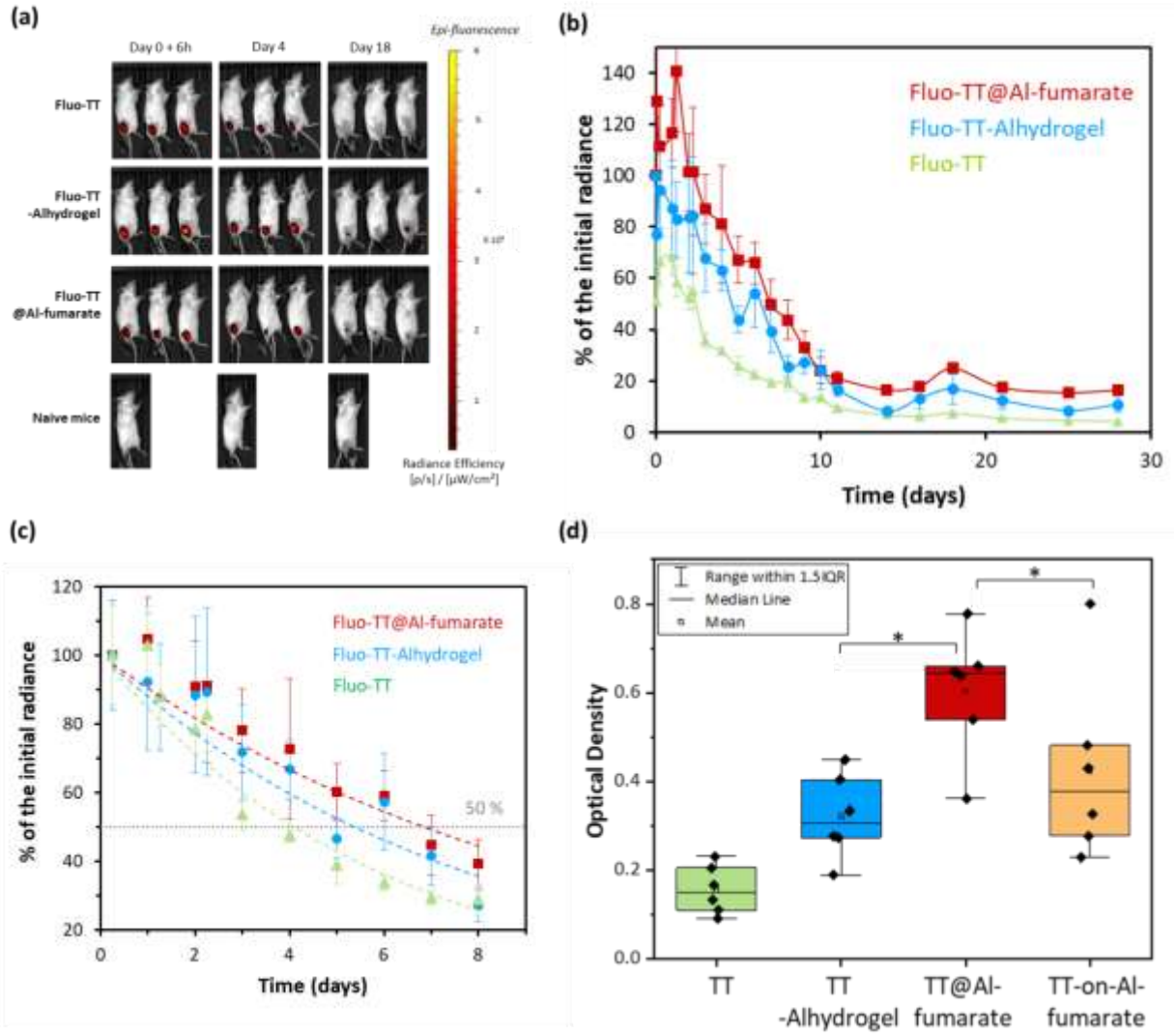

Figure 4. (a) *Evolution of NIR fluorescence signal in vivo after injection of fluo-TT, fluo-TT-Alhydrogel and fluo-TT@Al-fumarate after 6 h, 4 days and 18 days (50 µl, IM, quadriceps).* ***(b)*** *Longitudinal study of the fluorescence radiance with normalized signal to 100 % based on the value measured at t = 0. Error bars represent standard error of the mean.* ***(c)*** *Decay of the fluorescence radiance during 8 days, with the radiance signal normalized to 100 % based on the value measured at t = 6 h. Error bars represent the standard error of the mean.* ***(d)*** *Anti-TT Ig response 32 days after immunization (20 µl, IM, right hind-limb) with, from left to right, TT, TT-Alhydrogel, TT@Al-fumarate and TT-on-Al-fumarate. All formulations contain same TT and Al contents (Table S10). Boxes 25-75 percentiles, diamond shapes represent individual mice. *p < 0.05 as determined via Tukey's correction as part of a one-way ANOVA.*

Co-immobilization with an immune orienteer

In one-shot immunisation experiments, similar negligible amount of IgA was observed using either TT@Al-fumarate or TT-Alhydrogel, in agreement with Al-based adjuvants limitation to solely induce humoral response.[14] To examine the possibility of modulating the TH1/TH2 balance, an immune orienteer, CpG 1018 (phosphorothioate oligonucleotides, 22-mer), already approved in human vaccines,[74] was added in the TT@Al-fumarate formulation.

CpG 1018 was directly immobilized together with the TT antigen within Al-fumarate without hampering the MOF formation (Fig. 5a). Phosphorous was used as a probe element of CpG 1018 and was detected only in CpG1018@Al-fumarate and CpG1018+TT@Al-fumarate samples and not in the synthesis supernatants (Table S11), confirming CpG 1018 immobilization. Upon Al-fumarate degradation (in PBS/EDTA solution), CpG 1018 was released and its integrity was confirmed by electrophoresis in 5 % agarose gel (Fig. 5b).

Vaccines were formulated at the C1 concentration, with 0.4 µg/µl CpG 1018 and identical aluminium content between the adjuvanted formulations (Table S12). Mice were immunized twice at D0 and D20 (Fig. 5c). After 42 days, low but significant amount of IgA anti-TT antibodies were only detected in sera of the CpG 1018 boosted TT@Al-fumarate group (Fig. 5d). A striking increase in IgG2a anti-TT antibodies as a surrogate marker of a cellular response shift was observed with CpG1018 boosted TT@Al-fumarate (Fig. 5e). Interestingly, some mice exhibited IgG2a as early as 20 days after one injection (Fig. S32).

In the present study, at aim of comparing IgG production using the reference and new adjuvants, no attempts have been done to check accurately cellular response, beyond IgG isotype switch induced by CpG 1018 as a fair surrogate marker of such response. However, the TH1/TH2 shift was observed using relatively low dose of CpG 1018 within TT@Al-fumarate (2*8 µg/mouse), 120 times less than the non-encapsulated 3000 µg in Human Heplisav-B vaccine,[74] suggesting high potential of Al-fumarate for vaccine formulation with low dose of immune orienteer also inducing cellular responses in addition to humoral responses.

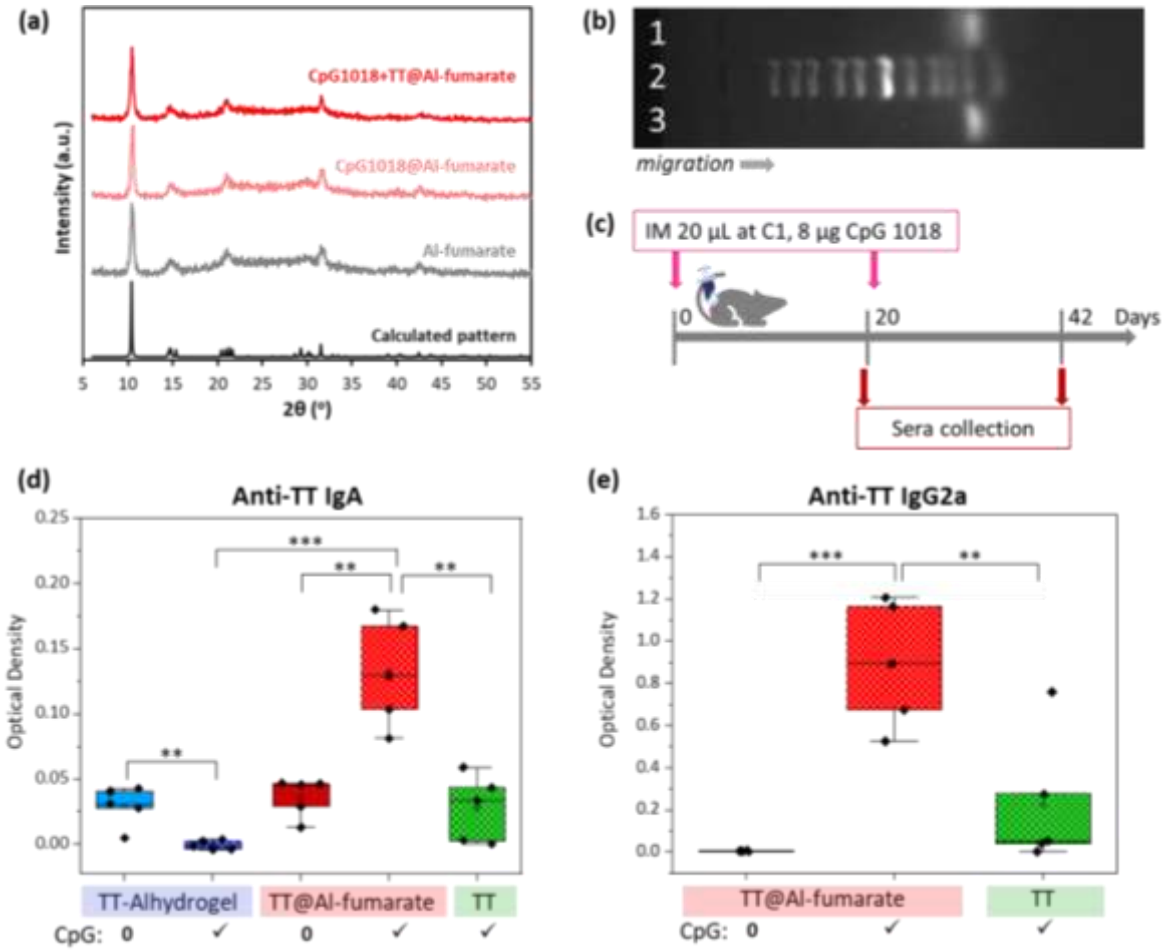

Figure 5. ***(a)*** *Powder X-Ray patterns of Al-fumarate calculated (obtained from CCDC, deposition number: 1051975, database identifier: DOYBEA), Al-fumarate, CpG1018@Al-fumarate, and CpG1018+TT@Al-fumarate.* λ = 1.5406 Å. ***(b)*** *Electrophoresis in 5 % agarose gel, lane 1: CpG 1018, lane 2: molecular weight ladder, lane 3: CpG 1018 released from Al-fumarate.* ***(c)*** *Mice vaccination study (N=5). All formulations contain same TT, CpG 1018, and Al contents (Table S12).* ***(d)*** *Anti-TT IgA response 42 days after IM immunization with, from left to right, TT-Alhydrogel, CpG1018+TT-Alhydrogel, TT@Al-fumarate, CpG1018+TT@Al-fumarate, and CpG1018+TT. N=5, Sera diluted to 1/100. Boxes 25-75 percentiles, **p < 0.01, ***p < 0.001 as determined via Tukey's correction as part of a one-way ANOVA.* ***(e)*** *Anti-TT IgG2a response 42 days after immunization with, from left to right, TT@Al-fumarate, CpG1018+TT@Al-fumarate and CpG1018+TT. Sera diluted to 1:1000. Boxes 25-75 percentiles, **p < 0.01, ***p < 0.001 as determined via Tukey's correction as part of a one-way ANOVA.*

Inactivated *E. coli* vaccines

To further demonstrate the universality of this novel adjuvant, another type of antigen for non-living vaccines, inactivated bacteria, much wider in size and with more complex structures than toxoids were also investigated. Very few reports concern the association of bacteria with MOFs. Mostly zinc imidazolate based or a Fe-polycarboxylate MOFs have been considered,[63,75–77] but to our knowledge, no Al-based system have previously been combined with bacteria. Formaldehyde inactivated *Escherichia coli* were selected as to date inactivated whole *E. coli* vaccines did not reach clinically efficient immunization, due to the poor *in vivo* stability of the immunogen.[63,78] The successful formation of inactivated *E.coli*@Al-fumarate was confirmed (Fig. S33). After MOF dissolution in PBS/EDTA solution, the analysis by flow cytometry revealed a different scatter profile for inactivated *E.coli*@Al-fumarate than non-encapsulated bacteria, suggesting their entrapment within the MOF matrix (Fig. 6a). On the other hand, bacteria liberated from Al-fumarate exhibited the same scatter profile as non-encapsulated bacteria, indicating their release without morphological damage. This was further confirmed by similar image aspect between non-encapsulated and released bacteria under single cell direct imaging.

Three inactivated *E. coli* vaccine formulations were prepared (inactivated *E. coli*, inactivated *E.coli*-Alhydrogel and inactivated *E.coli*@Al-fumarate) with comparable number of bacteria (ca $2.1.10^5$ bacteria/µl), and similar Al content for the adjuvanted formulations (Table S13). Mice were immunized twice (Fig. 6b). As shown in Fig. 6c, at D21, mice injected once with inactivated *E.coli*@Al-fumarate exhibited a strong Ig response whereas Ig levels were very low among inactivated *E.coli*-Alhydrogel and inactivated *E. coli* injected mice. At D42, mice from the inactivated *E.coli*@Al-fumarate group exhibited a higher Ig level, 3 times higher than without adjuvant and 1.6 higher than using the reference Al-adjuvant.

Al-fumarate is thus also suitable for the immobilization of inactivated bacteria, preserving their immunogenic potential and acting as an adjuvant leading to an enhanced immune response compared to bare inactivated bacteria and even to the reference Al-adjuvant.

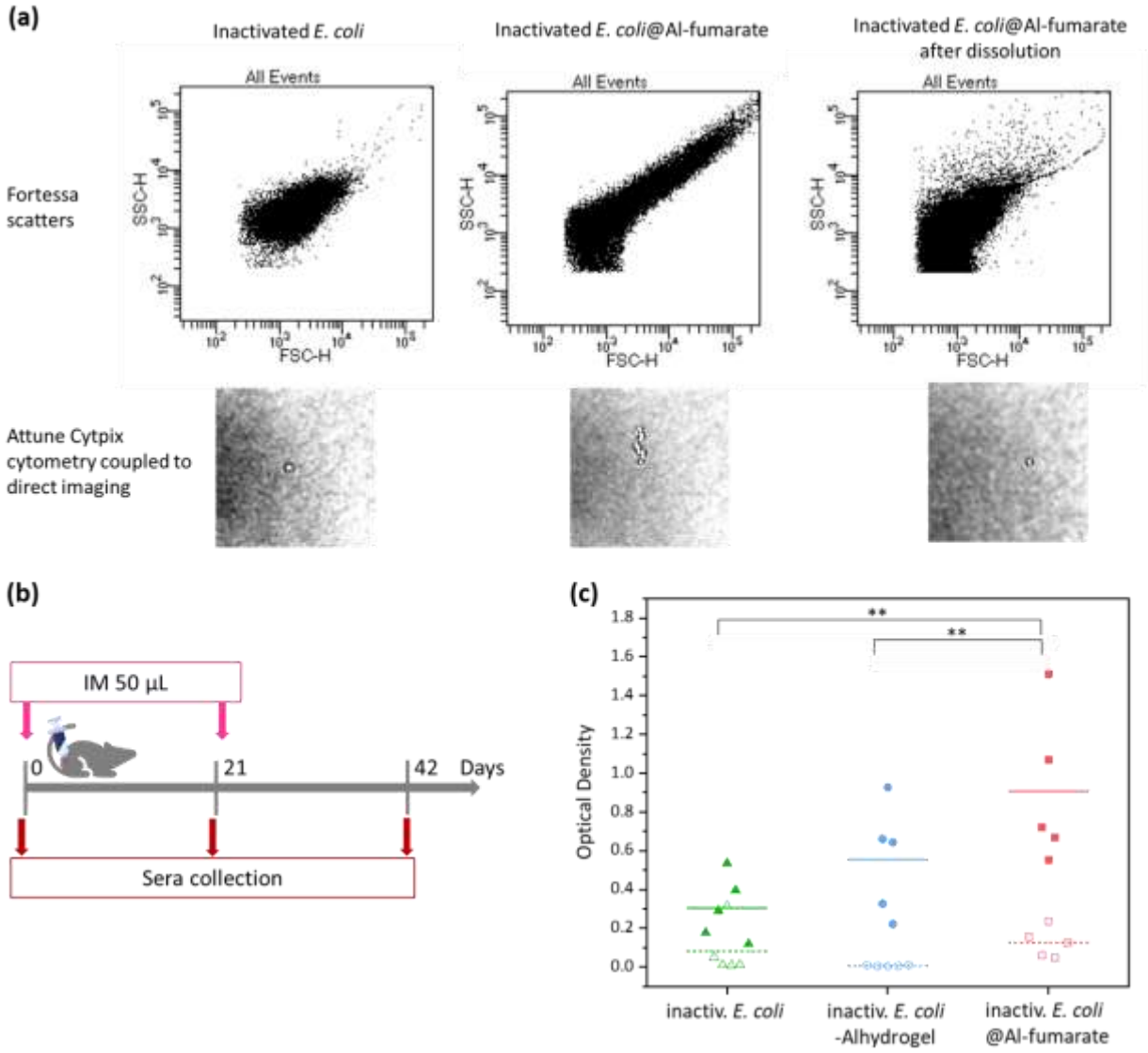

Figure 6. ***(a)*** *Flow cytometry analysis on inactivated E. coli (not immobilized, left), inactivated E.coli@Al-fumarate (middle), released inactivated E. coli from Al-fumarate (right); top row: axial and side scatters obtained on BD LSR Fortessa™ device; bottom row: direct video imaging performed using a Thermo Fisher Attune™ Cytpix™ on the bacteria gated on the scatters and SYTO 9 fluorophore detecting DNA from bacteria.* ***(b)*** *Mice vaccination study design (N=5). All formulations contain same E. coli and Al contents (Table S13).* ***(c)*** *Anti-E. coli Ig response 21 days (open symbols) and 42 days (full symbols) after IM immunization with, from left to right, inactivated E. coli, inactivated E.coli-Alhydrogel, inactivated E.coli@Al-fumarate. Sera diluted to 1:1000. **p < 0.01, as determined via Wilcoxon signed rank test. Bars represent mean value at days 21 (dashed) and 42 (plain). The atypical mouse in the inactivated E. coli group that exhibited a high antibody level at D21 had pre-immune level 2.7-fold higher than other mice suggesting a previous sensitization.*

Conclusions and outlooks

Although discovered one century ago and used with only minor changes from that time, Al-adjuvants remain the "unsung heroes" of vaccination, even sometimes confused with excipients, despite their mandatory use for non-living vector immunization. Here, we report that the Al-based Metal-Organic Framework, Al-fumarate, can be synthesized using a water, room temperature process compatible with the entrapment of a variety of bio-entities (toxoids, nucleic acids, bacteria). Al-fumarate acted as a fully resorbable adjuvant with an antigen slow release, working as a more potent adjuvant than the canonical Al-adjuvant, Alhydrogel. This promising novel adjuvant is not only inexpensive and easy to scale-up, but its stability over 24 months at 4 °C makes it particularly suitable for use in Low- and Medium-Income Countries.

Even though, the exact mechanism by which adjuvants act still remains not fully elucidated,[71–73] it can be proposed that the improved immune potency of the Al-fumarate adjuvant originates from the concurrent slow release of both TT and Al from TT@Al-fumarate optimally delivered to Antigen Presenting Cells (APC), as well as from protection against *in vivo* degradation.

The encapsulation within Al-fumarate allowed to easily combine relatively low dose of immune orienteer to modulate the immune response. The matrix effect of Al-fumarate entrapping biological molecules opens the opportunity to associate intimately mixture of antigens, immune orienteers, both to protect and optimally deliver the mixture.

It should also be kept in mind that when antibody response is only needed for vaccine efficiency, Al-adjuvants remain the best answer for avoiding most serious vaccine side-effects linked to cellular responses. Conversely, the short duration of anti-covid immunity induced by RNA vaccines stresses on the need for further advances in adjuvants towards a sustained immune response as provided by Al-adjuvants against toxoids.

Experimental Section

Extensive description of the experimental section is given in the Supplementary Information.

TT vaccines formulations

TT@Al-fumarate synthesis. Two TT@Al-fumarate vaccines C0 and C1 were prepared and C1 was used as stock for the C2 and C3 diluted vaccines. A solution of $Al_2(SO_4)_3$ (0.1 M) and a solution of fumaric acid (0.2 M) were mixed together in a 1:1 volume ratio. The solution of Tetanus Toxoid of 2.8 mg/ml purchased from Creative Biolabs was used directly for the preparation of the vaccines. A few seconds after mixing the two solutions, the tetanus toxoid solution was added to the reaction (8.4 µl for C0 and 10.5 µl for C1). The final mixture was left under stirring at room temperature for 8 h. Subsequently, the vaccines were centrifuged at 12 000 *g* for 3 min. Then, the solid was redispersed in HEPES buffer (20 mM, pH 7.4). The TT@Al-fumarate vaccines were kept at 4 °C for around 2 days until the *in vivo* studies.

TT-Alhydrogel (reference adjuvant). Alhydrogel 2 % purchased from InvivoGen was used directly for the preparation of the TT-Alhydrogel vaccines. Two TT-Al-Alhydrogel vaccines C0 and C1 were prepared and C1 was used as stock for the C2 and C3 diluted vaccines. In detail, 8.4 µl (for C0) or 10.5 µl (for C1) tetanus toxoid solution was diluted in 175 µl (C0) or 219 µl (C1) PBS buffer volume (10 mM, pH 7.4), followed by the addition of 58 µl (C0) or 73 µl (C1) of the Alhydrogel suspension. The mixture was pipetted up and down for 5 min, to allow the adsorption of the antigen, and finally, the remaining amount of PBS buffer was added. The TT@Alhydrogel vaccines were kept at 4 °C for around 2 days until the *in vivo* studies.

TT-on-Al-fumarate (surface immobilization). Al-fumarate was synthesized following the same procedure as TT@Al-fumarate but H_2O was added instead of TT. Then, Al-fumarate was redispersed in Milli-Q H_2O and TT solution (2.8 mg/ml) was added. After 16 h, TT-on-Al-fumarate was centrifuged at 12 000 *g* for 3 min, and the supernatant was removed. Finally, HEPES buffer (20 mM, pH 7.4) was added and the TT-on-Al-fumarate vaccine was kept at 4 °C, for *in vivo* studies.

CpG1018+TT vaccine formulations.

CpG 1018 (phosphorothioate oligonucleotides, 22-mer, TGACTGTGAACGTTCGAGATGA, modification: all bases) was obtained from Proteogenix in the powder form and directly used without further purification. 1051.83 µg CpG 1018 was dissolved in 35 µl of RNase-free H_2O.

For *CpG1018+TT@Al-fumarate*, the same procedure as for TT@Al-fumarate was followed, but with the addition of TT solution (2.8 mg/ml) and of the CpG 1018 solution (30 µg/µl).
For CpG1018+TT-Alhydrogel, the same procedure as for TT-Alhydrogel was followed, with the addition of the CpG 1018 solution (30 µg/µl).

Inactivated *E. coli* vaccine formulations.

Wild uropathogen *E. coli* strain with no antibiotic resistance was isolated from a urinary infection on CPSO agar. That local strain is available upon request to the authors. One *E. coli* colony was plated on TSA agar. Bulk bacterial culture dish was recovered and resuspended by flooding with 1 % aqueous solution of 37 % formaldehyde, 1 % BSA in PBS buffer (0.150 mM, pH 7.4). The inactivated *E. coli* suspension was kept ~ 4 °C until use. Prior to immobilization the inactivated *E. coli* suspension was washed twice with NaCl 0.9 % (2 400 g, 5 min). The resulting suspension was adjusted in order to contain ca 7-8x10^6 bacteria/µl (determined by flow cytometry).
For Inactivated E.coli@Al-fumarate vaccine and Inactivated E.coli-Alhydrogel vaccine. The same procedure than for the TT vaccine was followed but with the addition of inactivated *E. coli* suspension (ca 7.5x10^6 bacteria/µl) instead of TT solution. The suspension was kept at 4 °C, until the in vivo studies.

Animal studies

Ethics statement. All animal studies were done in accordance with protocol part of project n° APAFiS# 15557-2018061813422925_v3 which was submitted to the VOXCAN ethical committee (CEAA-129) and the French authorities (ministry of national education, the higher education and research) and received a favourable opinion on 22-JUN-2018 and 26-JUN-2018, respectively.
For all studies, mice were housed collectively in disposable standard cages in ventilated racks under a controlled temperature of 21 ± 3 °C, humidity between 30-70 %, with a light cycle of 12 h of light / 12 h of dark. Filtered water and autoclaved standard laboratory food for rodent were provided ad libitum. Prior to vaccine administration mice were anaesthetised under volatile anaesthesia (isoflurane and oxygen as a carrier gas).
For all studies, just before animal administration, the vaccines were kept at room temperature for a few minutes to avoid administering a cold solution. Prior to injection, right before filling the syringe, each vaccine was carefully re-suspended by vortex. For all studies, injections were done with 26G disposable needles placed on 50 µl Hamilton syringes.

TT immunization studies. In a typical experiment (details of each immunisation study can be found in the Supplementary Information), seven weeks old Balb/c female mice of 18 to 21 g were immunized by intra-muscular injection in the quadriceps muscle of the right hind leg with 20 µl of the tested formulations (either TT, TT-Alhydrogel, TT@Al-fumarate or TT-on-Al-fumarate) with a constant ratio of TT/Al^{3+} = 0.08 IU/µg Al for Al-adjuvanted formulations. For each formulation, 5 or 6 mice were used per group and sacrificed at 7, 14, 30 or 60 days after injection depending on the study.

High doses TT immunization study. Seven weeks old Balb/c female mice of ~ 21 g were immunized by intra-muscular injection in both hind-limb with 50 µl and by subcutaneous (SC) in the right flank with 100 µl of formulations at the C1 concentration. The mice were thus in total injected with 200 µl at the C1 concentration. Euthanasia was performed at 7 days (1 mouse), 32 days (2 mice), 60 days (2 mice) and 90 days (2 mice) after injections.

CpG 1018 + TT immunization study. Seven weeks old Balb/c female mice of ~ 19 g were immunized by intra-muscular injection in the right hind-limb with 20 µl of either TT+CpG1018, TT-Alhydrogel, TT+CpG1018-Alhydrogel, TT@Al-fumarate or CpG1018+TT@al-fumarate. All vaccines were formulated at the C1 concentration and for the formulation containing CpG 1018 so that 8 µg CpG 1018 were injected. For each formulation, 10 mice were used per group and two additional mice were included in the study as a control group, which did not receive any vaccine injection (naive mice). Euthanasia was performed for half of the mice (N = 5) 20 days after the injection (D20) and for the remaining mice (N = 5) 42 days after injection (D42). One naïve mouse was sacrificed at D20 and 1 naïve mouse was sacrificed at D42. Twenty days after the injection, the remaining mice of each group, received another 20 µl intra-muscular injection in the quadriceps muscle of the right hind leg.

Inactivated E. coli immunization study. Seven weeks old Balb/c female mice of ~ 20 g were immunized by intra-muscular injection in the right hind-limb with 50 µl of either inactivated *E. coli*, inactivated *E.coli*@Al-fumarate or inactivated *E.coli*-Alhydrogel. Each vaccine was prepared to contain a comparable number of bacteria, with a constant ratio of Al, for both Al-fumarate and Alhydrogel adjuvants. For each formulation (inactivated *E. coli*, inactivated *E.coli*@Al-fumarate or inactivated *E.coli*-Alhydrogel) 10 mice were used per group and 3 additional mice were included in the study as a control group, which did not receive any vaccine injection (naive mice). Euthanasia was performed for half of the mice (N = 5) 21 days after the injection (D21) and for the remaining mice (N = 5) 42 days after injection (D42). 1 naïve mouse was sacrificed at 21 days after injection, and 2 naïve mice were sacrificed at 42 days. 21 days after the injection, the remaining mice of each group, received another 50 µl intra-muscular

injection in the quadriceps muscle of the right hind leg. At the start of the study (D0), blood was sampled by retro-orbital sinus route under anaesthesia.

Antibodies responses

Sera were analysed for whole antibodies (Ig) responses using an anti-mouse light chain ELISA, for IgG antibodies responses using an anti-mouse IgG specific ELISA, and for IgA using an anti-alpha chain specific antibody. In one experiment Ig isotypes IgG1, IgG2a and IgG2b were also measured. ELISA was performed according to the manufacturer's instruction (alpha Diagnostic International). Special attention was paid to use conditions allowing an accurate comparison of antibodies titers: sera were tested on the same microtiter plate allowing direct OD comparisons, or at the same time on several plates, with an identical reference curve on each plate allowing correcting OD values. Correction was usually of 1 % and no more than 5 %.

Evaluation of the Al content at the injection site

The resorptive character of the TT@Al-fumarate formulation was evaluated by quantifying the amounts of remaining Al^{3+} at the injection sites of mice (right hind-limb) immunized with Al-fumarate based vaccine and compared to that of the non-resorptive TT-Alhydrogel.

At euthanasia, the limbs were harvested and fixed in 4 % PFA in HEPES buffer 20 mM pH 7.4. HEPES buffer was selected to ensure no degradation of the MOF could occur afterward.

The presence of Al^{3+} (deriving from the two adjuvants) at the injection sites (right limbs) was investigated via ICP-OES. The left limbs of all samples, as well as both limbs of all mice injected with only TT and both limbs of naïve mice were also analysed by ICP-OES, as negative controls. The fixation medium (PFA) was also analysed to ensure that no MOF degradation and subsequent Al^{3+} leaching occurred during the fixation protocol. Al^{3+} was never detected in any of the fixation media.

Digestion procedure for limb samples: All limb samples were removed from their storage media and were dehydrated at 100 °C for 5 h before treatment. After dehydration, the limbs were pre-digested with 2.5 ml HNO_3 (70 %, analytical grade) for 3 days at RT, followed by a total digestion at 50 °C for 3 h. For the ICP analysis, all digested samples were diluted to a final volume of 20 ml, using Milli-Q H_2O.

Acknowledgments

The authors thanks C. Livage for MEB experiments, A. Damond for HPLC experiments, C. Terryn for confocal laser microscopy images. M. Joiner and S. Behar from ThermoFisher for access and experiments on the Thermo Fisher Attune™ Cytpix™. The Plateau technique de Microscopie Electronique du Muséum National d'Histoire Naturelle is acknowledged. This work was done within the C2N micro nanotechnologies platforms and partly supported by the RENATECH network. Part of this work was supported by a public grant overseen by the French National Research Agency as part of the "Investissements d'Avenir" program (Labex Charm3at, ANR-11-LABX-0039-grant). I.C., E.G., J.H.M.C. and C.S. deeply thank the SATT Paris-Saclay for support and funding.

Author contribution

I.C. and E.G. contributed equally. J.H.M.C. and C.S. conceived, guided the project, and acquired funding. I.C., E.G., and B.R. contributed to the conceptual design of the study. I.C., E.G., F.B., M.H., N.S., and C.S. performed experiments, data analysis or conceptualisation on the MOF materials. G.P. and C.D. performed electronic microscopy studies. A.P-M. performed histological analysis. C.L., M.L., and E.C. performed the mice immunization studies. S.A. performed the flow cytometry analysis. B.R., A.K, T.T., and J.H.M.C. performed experiments, data analysis or conceptualisation of the biological studies. I.C., E.G., J.H.M.C., and C.S. wrote the paper. All authors edited versions of the manuscript, read, and approved the final manuscript.

Conflict of Interest

E.G., J.H.M.C., and C.S. are inventors of a patent application that describes the use of Al-MOF as a vaccine adjuvant.

References

1. Pollard, A. J. & Bijker, E. M. A guide to vaccinology: from basic principles to new developments. *Nat Rev Immunol* **21**, 83–100 (2021).
2. Poland, G. A. & Kennedy, R. B. Vaccine safety in an era of novel vaccines: a proposed research agenda. *Nat Rev Immunol* **22**, 203–204 (2022).
3. O'Hagan, D. T. *Vaccine Adjuvants*. vol. 42 (Humana Press, 2000).

4. Di Pasquale, A., Preiss, S., Da Silva, F. T. & Garçon, N. Vaccine adjuvants: From 1920 to 2015 and beyond. *Vaccines* **3**, 320–343 (2015).
5. Glenny, A. T., Pope, C. G., Waddington, H. & Wallace, U. Immunological notes. XVII-XXIV. *J. Pathol.* **29**, 31–40 (1926).
6. HogenEsch, H., O'Hagan, D. T. & Fox, C. B. Optimizing the utilization of aluminum adjuvants in vaccines: you might just get what you want. *npj Vaccines* **3**, 1–11 (2018).
7. He, P., Zou, Y. & Hu, Z. Advances in aluminum hydroxide-based adjuvant research and its mechanism. *Human Vaccines & Immunotherapeutics* **11**, 477–488 (2015).
8. Chong, H., Brady, K., Metze, D. & Calonje, E. Persistent nodules at injection sites (aluminium granuloma)-clinicopathological study of 14 cases with a diverse range of histological reaction patterns. *Histopathology* **48**, 182–188 (2006).
9. Verdier, F. *et al.* Aluminium assay and evaluation of the local reaction at several time points after intramuscular administration of aluminium containing vaccines in the Cynomolgus monkey. *Vaccine* **23**, 1359–1367 (2005).
10. Goto, N. & Akama, K. Histopathological Studies of Reactions in Mice Injected with Aluminum-Adsorbed Tetanus Toxoid. *Microbiology and Immunology* **26**, 1121–1132 (1982).
11. Vecchi, S., Bufali, S., Skibinski, D. A. G., O'hagan, D. T. & Singh, M. Aluminum Adjuvant Dose Guidelines in Vaccine Formulation for Preclinical Evaluations. *Journal of Pharmaceutical Sciences* **101**, 17–20 (2012).
12. Alfrey, A. C., LeGendre, G. R. & Kaehny, W. D. The Dialysis Encephalopathy Syndrome: Possible Aluminum Intoxication. *N Engl J Med* **294**, 184–188 (1976).
13. Berend, K., Van Der Voet, G. & Boer, W. H. Acute aluminum encephalopathy in a dialysis center caused by a cement mortar water distribution pipe. *Kidney International* **59**, 746–753 (2001).
14. Lindblad, E. B. Aluminium compounds for use in vaccines. *Immunol Cell Biol* **82**, 497–505 (2004).
15. Moyer, T. J. *et al.* Engineered immunogen binding to alum adjuvant enhances humoral immunity. *Nat Med* 430–440 (2020) doi:10.1038/s41591-020-0753-3.
16. Kumru, O. S. *et al. Effects of aluminum-salt, CpG and emulsion adjuvants on the stability and immunogenicity of a virus-like particle displaying the SARS-CoV-2 receptor-binding domain (RBD).* http://biorxiv.org/lookup/doi/10.1101/2023.07.10.548406 (2023) doi:10.1101/2023.07.10.548406.

17. Otto, R. B. D., Burkin, K., Amir, S. E., Crane, D. T. & Bolgiano, B. Patterns of binding of aluminum-containing adjuvants to Haemophilus influenzae type b and meningococcal group C conjugate vaccines and components. *Biologicals* **43**, 355–362 (2015).
18. McKee, A. S. & Marrack, P. Old and new adjuvants. *Current Opinion in Immunology* **47**, 44–51 (2017).
19. Facciolà, A., Visalli, G., Laganà, A. & Di Pietro, A. An Overview of Vaccine Adjuvants: Current Evidence and Future Perspectives. *Vaccines* **10**, 819 (2022).
20. Petroski, N. Advax Adjuvant. in *Immunopotentiators in Modern Vaccines* 199–210 (Elsevier, 2017). doi:10.1016/B978-0-12-804019-5.00010-4.
21. Micoli, F. & MacLennan, C. A. Outer membrane vesicle vaccines. *Seminars in Immunology* **50**, 101433 (2020).
22. Naumann, K. *et al.* Activation of Dendritic Cells by the Novel Toll-Like Receptor 3 Agonist RGC100. *Clinical and Developmental Immunology* **2013**, 1–11 (2013).
23. Firmino-Cruz, L. *et al.* Intradermal Immunization of SARS-CoV-2 Original Strain Trimeric Spike Protein Associated to CpG and AddaS03 Adjuvants, but Not MPL, Provide Strong Humoral and Cellular Response in Mice. *Vaccines* **10**, 1305 (2022).
24. Sabanovic, B., Piva, F., Cecati, M. & Giulietti, M. Promising Extracellular Vesicle-Based Vaccines against Viruses, Including SARS-CoV-2. *Biology* **10**, 94 (2021).
25. Hutter, J. N. *et al.* First-in-human assessment of safety and immunogenicity of low and high doses of Plasmodium falciparum malaria protein 013 (FMP013) administered intramuscularly with ALFQ adjuvant in healthy malaria-naïve adults. *Vaccine* **40**, 5781–5790 (2022).
26. Young Chung, J. *et al.* Vaccination against SARS-CoV-2 using extracellular blebs derived from spike protein-expressing dendritic cells. *Cellular Immunology* **386**, 104691 (2023).
27. Ahuja, R., Srichandan, S., Meena, J., Biswal, B. K. & Panda, A. K. Immunogenicity Evaluation of Thermostable Microparticles Entrapping Receptor Binding Domain of SARS-CoV-2 by Single Point Administration. *Journal of Pharmaceutical Sciences* **112**, 1664–1670 (2023).
28. Peng, S. *et al.* Particulate Alum via Pickering Emulsion for an Enhanced COVID-19 Vaccine Adjuvant. *Adv. Mater.* **32**, 2004210 (2020).
29. Pulendran, B., S. Arunachalam, P. & O'Hagan, D. T. Emerging concepts in the science of vaccine adjuvants. *Nat Rev Drug Discov* **20**, 454–475 (2021).

30. Reed, S. G., Orr, M. T. & Fox, C. B. Key roles of adjuvants in modern vaccines. *Nat Med* **19**, 1597–1608 (2013).
31. Harandi, A. M. Systems analysis of human vaccine adjuvants. *Seminars in Immunology* **39**, 30–34 (2018).
32. Schijns, V. E. & Lavelle, E. C. Trends in vaccine adjuvants. *Expert Review of Vaccines* **10**, 539–550 (2011).
33. Zhang, Y. *et al.* Alum/CpG Adjuvanted Inactivated COVID-19 Vaccine with Protective Efficacy against SARS-CoV-2 and Variants. *Vaccines* **10**, 1208 (2022).
34. Ella, R. *et al.* Safety and immunogenicity of an inactivated SARS-CoV-2 vaccine, BBV152: interim results from a double-blind, randomised, multicentre, phase 2 trial, and 3-month follow-up of a double-blind, randomised phase 1 trial. *The Lancet Infectious Diseases* **21**, 950–961 (2021).
35. Yin, Q. *et al.* A TLR7-nanoparticle adjuvant promotes a broad immune response against heterologous strains of influenza and SARS-CoV-2. *Nat. Mater.* (2023)
36. Jiang, H., Alezi, D. & Eddaoudi, M. A reticular chemistry guide for the design of periodic solids. *Nature Reviews Materials* **6**, 466–487 (2021).
37. Bennett, T. D. & Horike, S. Liquid, glass and amorphous solid states of coordination polymers and metal–organic frameworks. *Nat Rev Mater* **3**, 431–440 (2018).
38. Wang, S. *et al.* DNA-Functionalized Metal–Organic Framework Nanoparticles for Intracellular Delivery of Proteins. *J. Am. Chem. Soc.* **141**, 2215–2219 (2019).
39. He, C., Lu, K., Liu, D. & Lin, W. Nanoscale Metal–Organic Frameworks for the Co-Delivery of Cisplatin and Pooled siRNAs to Enhance Therapeutic Efficacy in Drug-Resistant Ovarian Cancer Cells. *J. Am. Chem. Soc.* **136**, 5181–5184 (2014).
40. Linnane, E., Haddad, S., Melle, F., Mei, Z. & Fairen-Jimenez, D. The uptake of metal–organic frameworks: a journey into the cell. *Chem. Soc. Rev.* **51**, 6065–6086 (2022).
41. Hidalgo, T., Simón-Vázquez, R., González-Fernández, A. & Horcajada, P. Cracking the immune fingerprint of metal–organic frameworks. *Chem. Sci.* **13**, 934–944 (2022).
42. Chen, P. *et al.* Bioinspired Engineering of a Bacterium-Like Metal–Organic Framework for Cancer Immunotherapy. *Adv. Funct. Mater.* **30**, 2003764 (2020).
43. Zhang, H. *et al.* Site-specific MOF-based immunotherapeutic nanoplatforms via synergistic tumor cells-targeted treatment and dendritic cells-targeted immunomodulation. *Biomaterials* **245**, 119983 (2020).
44. Ning, W. *et al.* Imparting Designer Biorecognition Functionality to Metal-Organic Frameworks by a DNA-Mediated Surface Engineering Strategy. *Small* **14**, 1703812 (2018).

45. Ni, K. *et al.* A Nanoscale Metal–Organic Framework to Mediate Photodynamic Therapy and Deliver CpG Oligodeoxynucleotides to Enhance Antigen Presentation and Cancer Immunotherapy. *Angewandte Chemie Intl Edit* **59**, 1108–1112 (2020).

46. Fan, Z. *et al.* Reversing cold tumors to hot: An immunoadjuvant-functionalized metal-organic framework for multimodal imaging-guided synergistic photo-immunotherapy. *Bioactive Materials* **6**, 312–325 (2021).

47. Wang, Z. *et al.* Organelle-Specific Triggered Release of Immunostimulatory Oligonucleotides from Intrinsically Coordinated DNA–Metal–Organic Frameworks with Soluble Exoskeleton. *J. Am. Chem. Soc.* **139**, 15784–15791 (2017).

48. Zhang, Y. *et al.* Metal-Organic-Framework-Based Vaccine Platforms for Enhanced Systemic Immune and Memory Response. *Advanced Functional Materials* (2016).

49. Duan, F. *et al.* A simple and powerful co-delivery system based on pH-responsive metal-organic frameworks for enhanced cancer immunotherapy. *Biomaterials* **122**, 23–33 (2017).

50. Yang, Y. *et al.* Reduction-Responsive Codelivery System Based on a Metal–Organic Framework for Eliciting Potent Cellular Immune Response. *ACS Appl. Mater. Interfaces* **10**, 12463–12473 (2018).

51. Miao, Y. B. *et al.* Engineering a Nanoscale Al-MOF-Armored Antigen Carried by a "Trojan Horse"-Like Platform for Oral Vaccination to Induce Potent and Long-Lasting Immunity. *Advanced Functional Materials* **29**, 1–10 (2019).

52. Zhong, X. *et al.* An aluminum adjuvant-integrated nano-MOF as antigen delivery system to induce strong humoral and cellular immune responses. *Journal of Controlled Release* **300**, 81–92 (2019).

53. Qi, Y. *et al.* Antigen-enabled facile preparation of MOF nanovaccine to activate the complement system for enhanced antigen-mediated immune response. *Biomater. Sci.* **7**, 4022–4026 (2019).

54. Zhao, H. *et al.* Nanoscale Coordination Polymer Based Nanovaccine for Tumor Immunotherapy. *ACS Nano* **13**, 13127–13135 (2019).

55. Li, X., Wang, X., Ito, A. & Tsuji, N. M. A nanoscale metal organic frameworks-based vaccine synergises with PD-1 blockade to potentiate anti-tumour immunity. *Nat Commun* **11**, 3858 (2020).

56. Zhang, G. *et al.* Poly(ethylene glycol)-Mediated Assembly of Vaccine Particles to Improve Stability and Immunogenicity. *ACS Appl. Mater. Interfaces* **13**, 13978–13989 (2021).

57. Cai, Z. *et al.* Photodynamic Therapy Combined with Antihypoxic Signaling and CpG Adjuvant as an In Situ Tumor Vaccine Based on Metal–Organic Framework Nanoparticles to Boost Cancer Immunotherapy. *Adv. Healthcare Mater.* **9**, 1900996 (2020).

58. Chen, P.-M. *et al.* Pollen-Mimetic Metal–Organic Frameworks with Tunable Spike-Like Nanostructures That Promote Cell Interactions to Improve Antigen-Specific Humoral Immunity. *ACS Nano* **15**, 7596–7607 (2021).

59. Stillman, Z. S., Decker, G. E., Dworzak, M. R., Bloch, E. D. & Fromen, C. A. Aluminum-based metal–organic framework nanoparticles as pulmonary vaccine adjuvants. *J Nanobiotechnol* **21**, 39 (2023).

60. Liang, K. *et al.* Biomimetic mineralization of metal-organic frameworks as protective coatings for biomacromolecules. *Nat Commun* **6**, 7240 (2015).

61. Luzuriaga, M. A. *et al.* Enhanced Stability and Controlled Delivery of MOF-Encapsulated Vaccines and Their Immunogenic Response In Vivo. *ACS Appl. Mater. Interfaces* **11**, 9740–9746 (2019).

62. Singh, R. *et al.* Biomimetic metal-organic frameworks as protective scaffolds for live-virus encapsulation and vaccine stabilization. *Acta Biomaterialia* **142**, 320–331 (2022).

63. Luzuriaga, M. A. *et al.* Metal–Organic Framework Encapsulated Whole-Cell Vaccines Enhance Humoral Immunity against Bacterial Infection. *ACS Nano* **15**, 17426–17438 (2021).

64. Alvarez, E. *et al.* The structure of the aluminum fumarate metal-organic framework A520. *Angewandte Chemie - International Edition* **54**, 3664–3668 (2015).

65. Ettlinger, R. *et al.* Toxicity of metal–organic framework nanoparticles: from essential analyses to potential applications. *Chem. Soc. Rev.* **51**, 464–484 (2022).

66. Gaab, M., Trukhan, N., Maurer, S., Gummaraju, R. & Müller, U. The progression of Al-based metal-organic frameworks – From academic research to industrial production and applications. *Microporous and Mesoporous Materials* **157**, 131–136 (2012).

67. World Health Organization. *The immunological basis for immunization series: module 3: tetanus*. (World Health Organization, 2018).

68. Manual for quality control of diphtheria, tetanus, pertussis and combined vaccines. https://www.who.int/publications-detail-redirect/WHO-IVB-11.-11.

69. McKee, A. S. *et al.* Alum Induces Innate Immune Responses through Macrophage and Mast Cell Sensors, But These Sensors Are Not Required for Alum to Act As an Adjuvant for Specific Immunity. *The Journal of Immunology* **183**, 4403–4414 (2009).

70. Hutchison, S. *et al.* Antigen depot is not required for alum adjuvanticity. *FASEB j.* **26**, 1272–1279 (2012).

71. Rimaniol, A.-C. *et al.* Aluminum hydroxide adjuvant induces macrophage differentiation towards a specialized antigen-presenting cell type. *Vaccine* **22**, 3127–3135 (2004).

72. Marrack, P., McKee, A. S. & Munks, M. W. Towards an understanding of the adjuvant action of aluminium. *Nat Rev Immunol* **9**, 287–293 (2009).

73. Exley, C., Siesjö, P. & Eriksson, H. The immunobiology of aluminium adjuvants: how do they really work? *Trends in Immunology* **31**, 103–109 (2010).

74. European Medecines Agency. Heplisav B. https://www.ema.europa.eu/en/medicines/human/EPAR/heplisav-b.

75. Liang, K. *et al.* Metal-Organic Framework Coatings as Cytoprotective Exoskeletons for Living Cells. *Advanced Materials* **28**, 7910–7914 (2016).

76. Permyakova, A. *et al. In Situ* Synthesis of a Mesoporous MIL-100(Fe) Bacteria Exoskeleton. *ACS Materials Lett.* **5**, 79–84 (2023).

77. Lee, H. *et al.* Cell-in-Catalytic-Shell Nanoarchitectonics: Catalytic Empowerment of Individual Living Cells by Single-Cell Nanoencapsulation. *Advanced Materials* **34**, 2201247 (2022).

78. Nesta, B. & Pizza, M. Vaccines Against Escherichia coli. in *Escherichia coli, a Versatile Pathogen* (eds. Frankel, G. & Ron, E. Z.) vol. 416 213–242 (Springer International Publishing, 2018).